Computer Modeling of Electrostatic Steering and Orientational Effects in Antibody-Antigen Association

Richard E. Kozack,*‡ Michael J. d'Mello,*§ and Shankar Subramaniam*‡

*National Center for Supercomputing Applications, ‡Department of Physiology and Biophysics and Beckman Institute for Advanced Science and Technology, University of Illinois at Urbana-Champaign, Urbana, Illinois 61801; and §Thinking Machines Corporation, Cambridge, Massachusetts 02142 USA

ABSTRACT Brownian dynamics simulations are performed to investigate the role of long-range electrostatic forces in the association of the monoclonal antibody HyHEL-5 with hen egg lysozyme. The electrostatic field of the antibody is obtained from a solution of the nonlinear Poisson-Boltzmann using the x-ray crystal coordinates of this protein. The lysozyme is represented as an asymmetric dumbbell consisting of two spheres of unequal size, an arrangement that allows for the modeling of the orientational requirements for docking. Calculations are done with the wild-type antibody and several point mutants at different ionic strengths. Changes in the charge distribution of the lysozyme are also considered. Results are compared with experiment and a simpler model in which the lysozyme is approximated by a single charged sphere.

INTRODUCTION

The recognition of a specific antigen by an antibody molecule is an important component of immune response. Recent investigations employing both experimental techniques and computational modeling indicate that the rate of association between antigen and antibody is diffusion limited. Stopped-flow spectrophotometric experiments on the monoclonal antibody 2B5 raised against cytochrome *c* yield a viscosity-dependent rate constant that is consistent with such behavior (Raman et al., 1992). More recently, this behavior has also been observed in the D1.3-lysozyme system (J. Foote, Fred Hutchinson Cancer Research Center, 1994 personal communication). In addition, Brownian dynamics computer simulations on a schematic antibody-antigen system yield association rates with the proper order of magnitude (Northrup and Erickson, 1992). Earlier theoretical arguments (Creighton, 1982), whereby the Schmoluchowski reaction rate for two diffusing spheres is multiplied by the probability that they will approach each other in the precise geometry required for docking, had suggested a much smaller rate. The key to the numerical result is the entrapment of the proteins upon collision by the surrounding solvent, allowing the antibody and antigen to reorient themselves during an encounter, thus making a reaction more likely (Northrup and Erickson, 1992).

Because a given antibody has a high affinity for its corresponding antigen, it is likely there exists a mechanism beyond random diffusive motion for enhancing the association rate. An interesting proposal has been put forth that hydrodynamic forces can help pull proteins of complimentary shape together as they approach each other in solution (Brune and Kim, 1994). Another way in which the reaction rate can be increased is through the action of long-range electrostatic forces, which can maneuver the two proteins into a configuration favorable for binding, a phenomenon known as electrostatic steering (Davis et al., 1991b). Evidence of this effect was found in the cytochrome *c*-antibody experiments (Raman et al., 1992), in which the reaction rates decreased with increasing ionic strength. Such a feature raises the possibility that the association rate can be altered by point mutations that change the long-range steering forces. This means that antibodies can be engineered with either increased or decreased affinities for a given antigen through rational alterations of their electrostatic charge distributions.

The purpose of this study is to model electrostatic steering through Brownian dynamics simulations for a specific antibody-antigen complex and thus simulate in a more realistic manner the rates of encounter. We extend a previous study of ours (Kozack and Subramaniam, 1993) in two important ways. First we implement a recently developed algorithm (Holst, 1993; Holst et al., 1994a, b) for solving the full nonlinear Poisson-Boltzmann equation for the electrostatic field generated by a protein rather than employing a linearized approximate form. This enables us to model the effects of electrolytic ions in the surrounding solvent more accurately. Second, and more importantly, we employ a model that includes the orientational aspects of antibody-antigen association, instead of modeling the antigen as a simple charged sphere. Whereas our earlier work focused on relative reaction rates induced by point mutations, the model system used here gives absolute reaction rates that are similar to those observed for antibody-antigen complexes. In this regard, the computations described here are the first simulations of antibody-protein association that include realistic electrostatic steering fields. It should be pointed out that modeling of the substrate in greater detail has been carried out in cytochrome association reactions (Northrup et al.,

Received for publication 22 August and in final form 6 December 1994.

Address reprint requests to Dr. Shankar Subramaniam, Department of Physiology and Biophysics, Beckman Institute for Advanced Science and Technology, University of Illinois at Urbana-Champaign, Urbana, IL 61801. Tel.: 217-244-4489; Fax: 217-244-2909; E-mail: shankar@uiuc.edu.

0006-3495/95/03/807/08 $2.00

1987, 1993). Calculations with such detailed models are being explored in the association of the antibody-antigen complex.

As before, the system chosen for study is the complex between the monoclonal antibody HyHEL-5 and hen egg lysozyme. A 2.8-Å resolution crystal structure of the complex is available (Sheriff et al., 1987), and this system has long been studied as a model for antigen-antibody interactions. Electrostatic forces are of considerable importance in this system. The lysozyme itself has a large positive charge of +8e, and the stability of the system is mediated by three salt bridges involving residues Glu-H35 and Glu-H50 from the antibody and Arg-45 and Arg-68 of the lysozyme. Thermodynamic measurements show that the association enthalpy for the proteins is large and negative (Hibbits, et al., 1994). In addition, work with both natural (Smith-Gill et al., 1982) and designed (Lavoie et al., 1989) lysozyme mutants indicates that even conservative mutations of the abovementioned Arg residues can have a dramatic impact on the binding affinity of the two proteins. On the theoretical side, both free-energy calculations (Slagle et al., in press) and the Brownian dynamics studies cited above (Kozack and Subramaniam, 1993) have demonstrated the significant role played by charged residues in the formation of the complex.

An outline of our study is as follows. The crystallographic atomic coordinates of the Fv portion of HyHEL-5 were used to generate a charge distribution, which was in turn inserted into the nonlinear Poisson-Boltzmann equation to determine its electrostatic steering field. The lysozyme, which was modeled as an asymmetric dumbbell of two charged spheres, underwent Brownian motion in the field of the antibody. This representation is computationally simple, yet sufficiently detailed to capture the specific orientational nature of antibody-antigen docking. Because the reaction rate was obtained from an average over a large number of independent diffusive trajectories, the simulations were especially suited for massively parallel architectures, and issues related to this topic are briefly discussed. The enhancement of the association rate from electrostatic steering was investigated for the wild-type system and the effect of using the full nonlinear Poisson-Boltzmann equation for the electrostatic portion of the calculation was considered. Simulations for various solvent viscosities and ionic strengths were performed, and the results were compared with the 2B5-cytochrome *c* data. The effects of mutations are modeled both by varying the charge distribution of the model lysozyme and by making alterations of charged and uncharged residues on the antibody. This demonstrates how changes in the electrostatic properties of the systems are reflected in the reaction rate and allows us to address questions relevant to the design of more efficient antibodies.

MATERIALS AND METHODS

Brownian dynamics simulations

Brownian dynamics is a well established technique for modeling diffusion-controlled biomolecular reactions (Allison et al., 1988; Davis et al., 1991b; Getzoff et al., 1992; Northrup, 1994) and, in contrast with more commonly used molecular dynamics simulations, allows one to probe time scales of experimental interest. The simplification that makes this possible is the treatment of the solvent as a continuum both in terms of its electrostatic properties and its effect on the relative motion of the proteins. The electrostatic steering field obeys the nonlinear Poisson-Boltzmann equation (Sharp, 1994) for the potential ϕ, which for a 1:1 electrolyte is

$$-\nabla \cdot \epsilon \nabla u + \epsilon \kappa^2 \sinh u = \frac{e\rho}{kT} \tag{1}$$

with the "dimensionless" potential u defined as

$$u = \frac{e\phi}{kT}, \tag{2}$$

where e is the elementary unit of charge and kT is the Boltzmann factor. The right side of Eq. 1 is linear in ρ, the charge density of the protein, and contains all of the crystallographic information. The second term on the left side of the equation is nonzero only in the region outside the protein and gives the modification of the potential by the solvent and the ionic medium. The quantity ϵ is the dielectric constant and κ is the inverse Debye length, which is proportional to the square root of the ionic strength I. The remaining gradient term in the Poisson-Boltzmann equation reflects its origin in Gauss' Law of Electrostatics.

Once the electrostatic potential has been obtained, its influence on Brownian motion is determined from an algorithm developed by Ermak and McCammon (1978), which is a discrete version of the Langevin equation. For a composite structure consisting of N particles, the displacement vector $\Delta\mathbf{r}$ has $3N$ degrees of freedom and is given by

$$\Delta\mathbf{r} = (kT)^{-1}D\mathbf{F}\Delta t + \mathbf{R}, \tag{3}$$

where Δt is the time step, D is the $3N \times 3N$ diffusion tensor, $\mathbf{F}$ is the force vector, and $\mathbf{R}$ is a $3N$-dimensional random vector satisfying certain statistical constraints. More generally, the above equation includes an additional term that depends on the spatial derivatives of D; however, this term identically vanishes for the types of hydrodynamic interactions assumed here. Typically, a Brownian dynamics simulation is initiated with the two reacting molecules separated by a distance b, beyond which the long-range electrostatic forces are spherically symmetrical. Then Eq. 3 is employed to generate a trajectory that is terminated when either a predetermined reaction condition is satisfied, or the intermolecular separation becomes greater than a second distance q, which is larger than b. Because of the appearance of the random force term, which partly represents the interaction of the proteins with the surrounding solvent, each trajectory is not fully deterministic, and thus many trajectories are run to obtain a reaction probability β. The experimentally measurable association rate k is then given by Northrup et al. (1984)

$$k = \frac{k_s(b)\beta}{1 - (1 - \beta)k_s(b)/k_s(q)}, \tag{4}$$

where $k_s(a)$ is the analytical result for the diffusion rates of a point particle to spheres of radius a which can be written as

$$k_s(a) = 4\pi D\left[\int_a^\infty \frac{\exp(U(r)/kT)}{r^2}\,dr\right]^{-1}, \tag{5}$$

where $U(r)$ denotes the longrange potential.

Model system

Below we describe the application of Brownian dynamics methods to the HyHEL-5-lysozyme complex with emphasis placed on how the present model differs from our earlier simulations of the same system. As was done previously, only the Fv fragment of the antibody is considered in the calculations. The atomic coordinates are taken from the x-ray structure and the shape of the protein is defined by assigning optimized parameters for liquid simulations radii (Jorgensen and Tirado-Rives, 1988) to each heavy atom.

The charge distribution is built up from 38 sites assigned to the Asp, Glu, Arg, and Lys residues and the N-termini, yielding an overall net charge of 0. The electrostatic potential around the protein is found by solving the full nonlinear Poisson-Boltzmann equation using the multigrid damped inexact Newton algorithm (Holst et al., 1994a, b). In the earlier study, we used a linearized approximation to Eq. 1. The differences between the linear and nonlinear models are explored in a subsequent section of the paper. To implement the multigrid-Newton algorithm, a finite-difference formulation of the Poisson-Boltzmann equation (Warwicker and Watson, 1982) is made on a cubic grid measuring 127 nodes on a side at 1 Å resolution. As was done previously, the grid is centered at the point where the diagonal moments of the electric quadrupole tensor vanish and the boundary condition on the outer faces is generated by assuming that each charge contributes to the potential as if it were an independent Debye-Hückel sphere of radius 2 Å. The electrostatic calculations were performed on a Convex 3880 with the resulting potential grids being transferred to other machines for the purpose of running Brownian trajectories.

The lysozyme, which undergoes diffusive motion in the force field of the antibody, is represented as an asymmetrical dumbbell consisting of two spheres. A rough superposition of this model is displayed in Fig. 1 over a stick representation of the actual Fv-lysozyme complex. The smaller sphere, which approximates the two salt link-forming Arg residues, has a radius of 4.0 Å and a charge of +2e. The larger sphere, which models the remaining bulk of the protein, is assigned a radius of 20.0 Å and a charge of +6e. The distance between the centers of the spheres is equal to 24 Å, or the sum of their radii. Except for one case indicated below, it is assumed that there are no hydrodynamic interactions between the spheres. The lysozyme is kept rigid during the trajectories by applying a line of centers technique (Luty et al., 1993), in which a constraining correction is applied along the vector between the spheres after each time step. In our previous simulations only the smaller sphere was used to represent the lysozyme, whereas the present model is more realistic and allows for a description of the strict orientational constraints in protein-protein docking. As mentioned above, this means that reasonable absolute values for the association rate can be obtained.

The initial antibody-lysozyme separation b and the termination distance q are taken to be 80 and 500 Å, respectively. The time step is variable depending on the relative separation with a minimum value of 0.5 ps. The reaction condition, defined in terms of the smaller lysozyme sphere and the δ carbon of Glu-H50, is met when the centers of these two atoms are within 6.5 Å of each other. This distance, which was chosen to accurately reflect protein-protein reaction rates, differs from the 8.5 Å that was used in the earlier simulations to give high reaction probabilities and hence better statistics. Because of the comparatively low reaction rate, many more trajectories are computed than in the single-sphere model to get acceptable statistical errors. At least 300,000 trajectories were run to get each data point that is presented; in most cases at least 500,000 trajectories were sampled, and in a few examples a million or more trajectories were sampled. This portion of the calculation was done either on an SGI Challenge machine at the National Center for Supercomputing Applications, in single-processor mode or as a massively-parallel problem on the CM-5 from Thinking Machines Corporation (Cambridge, MA).

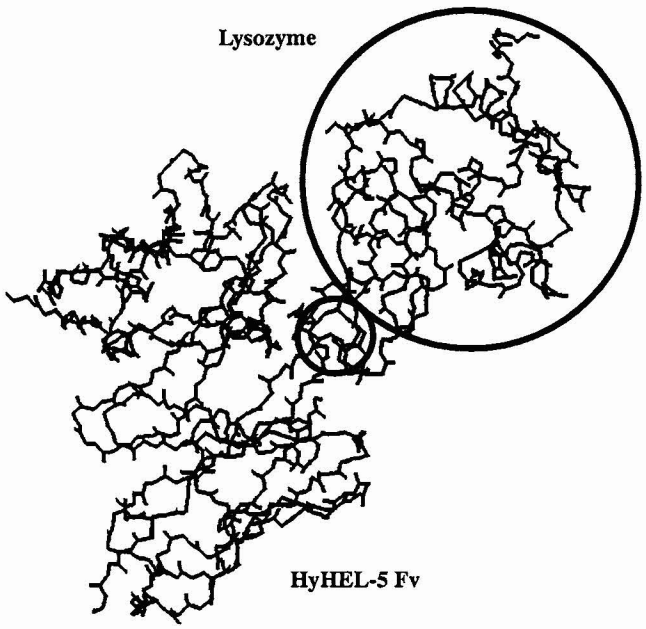

FIGURE 1 The two-sphere model of the lysozyme approximately superposed over a stick representation of the crystal structure for the Fv-lysozyme complex.

Computational issues

The UHBD software package (Davis et al., 1991a) provided the basis for our computations, although several key modifications of the code were made. One was implemented to enable the use of diffusing substrates that contain spheres of different sizes as in the asymmetric dumbbell model of the lysozyme. This was necessary to account correctly for simple collisions between antibody and antigen. A more extensive change involved the insertion of the multigrid-based Newton method for solving the nonlinear Poisson-Boltzmann, which has already been described in detail (Holst et al., 1994a). A final major modification required a reworking of the program for use on the CM-5. Other workers (Bagheri et al., 1993) have discussed the issue of parallelism with UHBD for machines with up to 10 processors. Below we concern ourselves with the deployment of the hundreds of processing nodes that are available on the CM-5.

Only the Brownian dynamics portion of the calculation has been run on the CM-5. Because this part of the code involves the running of many independent trajectories, it easily lends itself to parallelization on a large scale, and we have essentially followed a procedure similar to that for the more coarse-grained parallel machines (Bagheri et al., 1993). The basic outline of our program can be summarized in four steps. The electrostatic potential, which is efficiently calculated on a vector machine (Holst, 1993) such as the Convex and then transferred to the scalable disk array or even the front end disk of the CM-5, is first broadcast to all of the processors. Then a simple arithmetic expression based on the processor address number is used to locally modify the seed for the random number generator, which yields the stochastic force term in Eq. 4. As has been shown (Bagheri et al., 1993), this prescription leads to an independent set of the random numbers for each processor. In the third step, each of the nodes, which number m, runs a fixed number of trajectories N_t. Because each trajectory is made up of a variable number of time steps, there are differences in the work done by each node; these have been demonstrated to be small (Bagheri et al., 1993), and our experience is indeed in agreement with this. Finally, when all of the processors are done, the results from the total of mN_t trajectories are collected to find the reaction probability, which is then used to determine the rate constant.

It is shown in Fig. 2, for a series of runs with 32 processors, that the CPU time consumed in the Brownian dynamics simulations grows linearly with the total number of trajectories. The curve extrapolates to a nonzero value for zero trajectories due to overhead time required for reading in the force-field grid and tabulating the results of the run. We have also looked at the CPU time for eight different sets of random number seeds at 10 and 150 trajectories per processor and found the maximum deviation from the average to be <15% in each case. Presented in Fig. 3 is the CPU time required for running a fixed number of total trajectories with varying numbers of processors. As expected, this time decreases sharply with the number of processors. However, the speedup, defined as the CPU time for a 32-processor run divided by the CPU time for an m-processor run, scales less than linearly with m and ranges from 1.8 when the number of nodes is doubled from 32 to 64 to 6.2 for a 16-fold increase of processors. This is due to the increased importance of overhead time as the number of trajectories per processor decreases. It should be noted that the total number of trajectories has been chosen to specifically emphasize this feature, and one can obtain better speedups by simply running more trajectories. However, this exercise shows how the efficiency of the calculation is limited by the

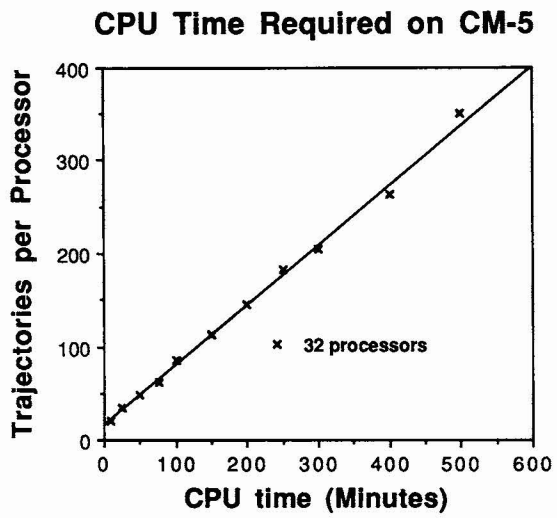

FIGURE 2 The CPU time required to run a variable number of trajectories on 32 processors of the CM-5. The y axis indicates the number of trajectories per processing node, and the straight line represents a least-squares linear fit to the data. The overhead time necessary to set up the problem and collect the results has been included.

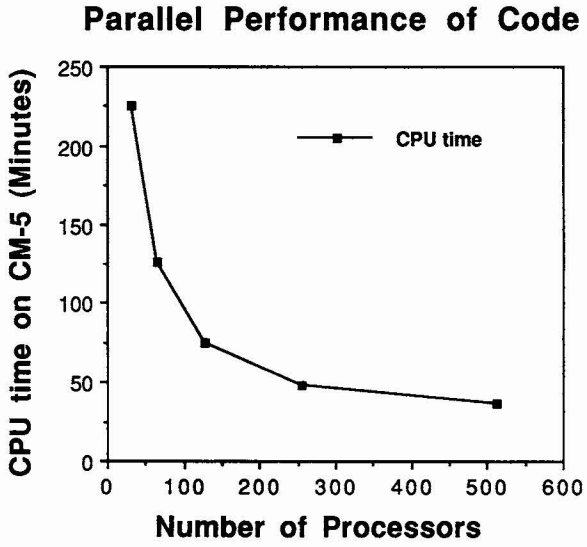

FIGURE 3 The CPU time required to run a total 10,240 trajectories of various numbers of processors on the CM-5. Each square represents actual timings, and the lines connecting the points are only for clarity. The overhead time necessary to set up the problem and collect the results has been included.

non-parallelizable portions of the program. This difficulty can be minimized with an efficient parallel implementation of a Poisson-Boltzmann solver, as this can eliminate the input/output step of reading in the potential grid.

RESULTS

Wild-type system

Simulations were performed for the wild-type system with electrostatic potentials calculated at ionic strengths of 5, 50, and 150 mM corresponding to Debye lengths of 43, 14, and 8 Å, respectively. The results are collected in Table 1 for

TABLE 1 Antibody-antigen association rates

Ionic Strength	Experiment	Nonlinear	Linear
5 mM	1×10^6	8.6×10^6	4.8×10^7
50 mM	6×10^5	2.4×10^6	7.3×10^6
150 mM	4×10^5	1.7×10^6	2.4×10^6
No steering	3×10^5	8.0×10^5	8.0×10^5

Comparison of calculated and observed antibody-antigen association rates in units of $M^{-1}\ s^{-1}$. The first column is the experimental data for the 2B5-cytochrome c system cited in the text, the second column is the simulation for the model HyHEL-5-lysozyme system where the nonlinear Poisson-Boltzmann equation has been used to calculate the steering field, and the third column is the same as the second except that the linearized approximation to the Poisson-Boltzmann equation is used. The "no steering" row indicates that electrostatic fields are not employed in the computations, and for the experiment means that an ionic strength of 1000 mM was used. The experimental results, given to one significant figure, were estimated from a graph, and the error in the simulated rates is on the order of 10%.

computations in which both the full nonlinear and the linearized Poisson-Boltzmann equations are used to obtain the steering field. Measurements for the 2B5-cytochrome c association rates (Raman et al., 1992) are also shown. As noted above, the reaction probabilities in the model computations are small and thus the statistical error inherent in the simulation is relatively large, on the order of 10%. The experimental data points have been estimated from a graph and are therefore listed to one significant figure. The "no steering" values are found experimentally by using an extremely high ionic strength and numerically by simply turning off the electrostatic steering force.

The computed reaction rate decreases with ionic strength, indicative of favorable electrostatic steering. The rates for the nonlinear calculation are roughly the same magnitude as, although a bit higher than, the corresponding experimental results. The variation in the rate with respect to ionic strength is greater for the simulated antibody-lysozyme system. These discrepancies could be due to specific features of the different systems, approximations implied in the modeling, or perhaps a combination of both. It is also seen in Table 1 that the difference between the nonlinear and linear calculations is quite considerable at 5 mM, but decreases as the ionic strength drops to 50 and then to 150 mM. This agrees with expectations that the linearized approximation of the Poisson-Boltzmann equation improves with increasing salt concentration. These results also match those of previous studies in which it is found that the linearized equation tends to exaggerate the effects of electrostatic steering (Allison et al., 1989; Holst et al., 1994a). Finally, the results from the linear calculations are further from the observations than the nonlinear calculations. Hereafter, all of the reaction rates presented in this paper are determined by using the full nonlinear Poisson-Boltzmann equation.

Because the experimental results on the cytochrome c-antibody complex (Raman et al., 1992) and the D1.3-lysozyme system (J. Foote, personal communication) include studies of the viscosity dependence of the association rate, we have considered the effect of varying the viscosity in our

simulations. The effect on the reaction rate can be written as

$$k_o/k = A + B\eta_{rel}, \quad (6)$$

where A and B are constants, k_o is the reaction rate when the solvent is water, k is the reaction rate in the viscous medium, and η_{rel} is the ratio of the viscosity to that of water. The above-cited empirical results agree well with Eq. 6 when $A = 0$ and $B = 1$, which are values that would be expected for a diffusion-controlled reaction (Kramers, 1940). In Fig. 4 are the rates for the wild-type system at 5 mM ionic strength where the ratio of the viscosity to that of water η_{rel} ranges from 1.0 to 2.2. The error bars are estimated by assuming that the fractional error is equal to the square root of the number of trajectories that result in a reaction, a procedure followed for all the graphs in this paper. A least-squares fit to the function k_o/η_{rel} is also shown in Fig. 4 and can be seen to reproduce the trend of the data.

The aim of this investigation is to examine electrostatic steering in antibody-antigen docking from realistic fields; thus, no attempt has been made to calculate any steering forces due to hydrodynamic interactions between the proteins. A simple estimate that the hydrodynamic forces can be much stronger has been based on an electrostatic force between two dipolar proteins (Brune and Kim, 1994). However, from Brownian dynamics simulations it is generally found that the local field around the active site is what determines the amount of electrostatic steering relevant to the reaction rate. For example, bovine superoxide dismutase and its substrate have net charges of the same sign (Sines et al., 1990), and in the present case the antibody is electrically neutral, yet both systems exhibit substantial favorable electrostatic steering. As far as hydrodynamic interactions internal to a protein are concerned, we feel that our model lysozyme is too elementary to justify their detailed consideration. We did perform one simulation, without electrostatic forces, in which an Oseen tensor (Dickinson, 1985) is employed to describe hydrodynamic interactions between the two lysozyme spheres. This resulted in a rate constant that was larger only by about a factor of 2 over the case in which no hydrodynamic interactions were employed.

Lysozyme mutants

One of the most important applications of Brownian dynamics simulations is the assessment of the effect of mutations on the reaction rate. Even though the model lysozyme is quite simple, we can still examine how the association rate depends on its charge distribution. In Fig. 5 are the results of simulations where the charge has been altered on the smaller lysozyme sphere, which is meant to model the two Arg residues that form salt bridges in the antibody-antigen complex. The changes are mainly manifest at 5 mM ionic strength, where the rate is [2/3] of the wild-type value for a reduction of one charge unit and 1/5 of wild-type for a reduction of two charge units. At the higher ionic strengths, the rates are within roughly a factor of 2 of the wild-type results. It is interesting to note that, within the statistical error, there is little or no change in the rate constant in going from 50 to 150 mM and at these molarities, there is no noticeable difference when the sphere contains zero or one unit of charge. Experimental results on natural and artificial mutants on the other hand have shown that antibody-lysozyme affinity is extremely sensitive to mutations of the Arg residues (Smith-Gill et al., 1982; Lavoie et al., 1987). Thus far, neither this study nor previous ones (Kozack and Subramaniam, 1993; Slagle et al., 1994) based on continuum electrostatic models have been able to reproduce this behavior. It is clear that more theoretical work, especially with atomic-level models, needs to be done to gain an understanding of this phenomenon.

As expected, the reaction rates are much less dependent on the charge on the larger lysozyme sphere, which is farther

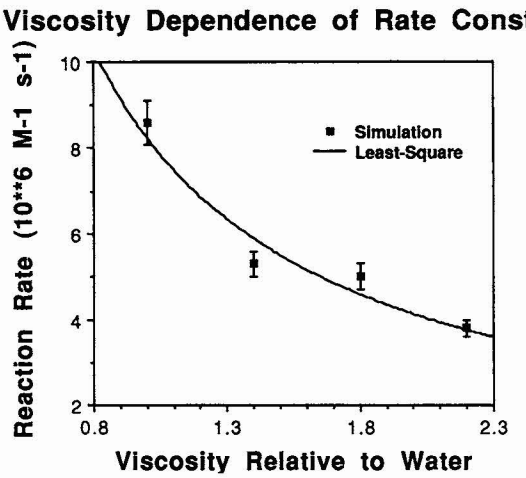

FIGURE 4 The rate constant for the wild-type model antibody-lysozyme system as a function of the solvent viscosity divided by the viscosity of water. The solid line is a least-squares fit to the function K/η where η is the viscosity.

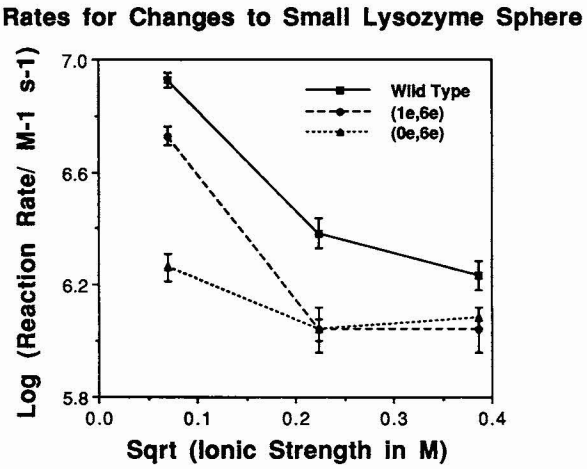

FIGURE 5 Reaction rates as a function of ionic strength for model systems in which the charge on the smaller lysozyme sphere is altered. The notation identifying the charges on each sphere is in order of (smaller, larger) so that (2e,6e) represents the wild-type system. The lines connecting the data points are for the sake of clarity.

from the reaction site. The results are given in Fig. 6. Even when the charge is neutralized from +6e, the rate decreases by only about a factor of 3 at 5 mM and even less so at higher salt concentrations. When the charge on this sphere is reduced by two units, the effect on the reaction rate is comparatively smaller and is virtually identical to the wild-type rates at 50 and 150 mM. This merely reflects what has been stated earlier, that local interactions near the binding site take precedence over the total charge of the molecule in determining the efficiency of electrostatic steering.

Antibody mutants

Since the model for the antibody is much more detailed, we can consider the effects of specific point mutations on antibody-antigen association. We have investigated a few representative cases that have had the largest impact in the single-sphere model. For mutations that decrease the reaction rate, these are the neutralizations of the Glu-H35 and the Glu-H50 residues, which form the salt links with the Arg-45 and Arg-68 residues of the lysozyme. The reaction rates are compared with those of the wild-type system in Fig. 7. The largest decrease is a factor of 5 for Glu-H50 at 5 mM ionic strength; otherwise the rates are within a factor of 2 from the wild-type complex. The relative rates, defined as the ratio of the reaction rate for the mutant system to that of the wild-type, are predicted remarkably well by the single-sphere lysozyme model at 5 mM. At higher salt concentration, the single-sphere model overestimates the effects of the mutations, although the corresponding relative rates have the same magnitude.

For mutations of HyHEL-5 that enhance the reaction rate, results are shown in Fig. 8 for Asn-to-Asp mutations at positions H59 and H100. The relative rates decrease with increasing ionic strength, which is contrary to the nonmonotonic behavior that was observed for the single-sphere model. The effect of the Asn-H100 mutation has disappeared at 150 mM, whereas the simpler model predicts a factor of 2 increase. Again the single-sphere model gives reasonable magnitudes for the relative rates, although it somewhat underestimates the low ionic strength rates. In particular, there is almost a fourfold increase for the Asn-H59 mutation at 5 mM, whereas the single-sphere model gave only a factor of 1.4 enhancements.

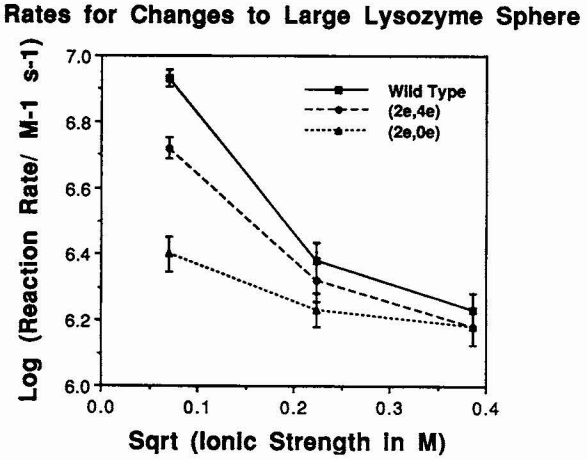

FIGURE 6 Reaction rates as a function of ionic strength for model systems in which the charge on the larger lysozyme sphere is altered. The notation identifying the charges on each sphere is in order of (smaller,larger) so that (2e,6e) represents the wild-type system. The lines connecting the data points are for the sake of clarity.

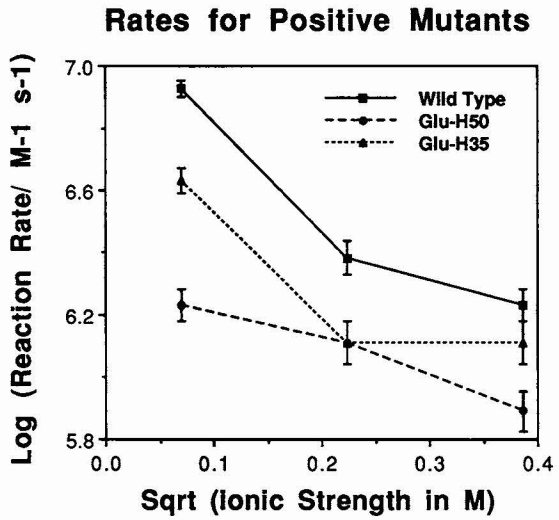

FIGURE 7 Reaction rates as a function of ionic strength for positive antibody mutants that decrease the amount of electrostatic steering. The lines connecting the data points are for the sake of clarity.

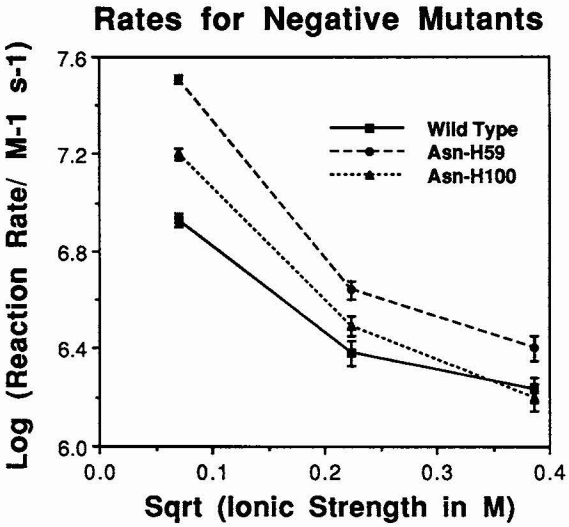

FIGURE 8 Reaction rates as a function of ionic strength for negative antibody mutants that increase the amount of electrostatic steering. The lines connecting the data points are for the sake of clarity.

DISCUSSION

For all of the mutations we have considered, both to the lysozyme and to the antibody, the observed reaction rates have been confined to the same order of magnitude as in the

wild-type system. This is in line with conclusions obtained in simulations of superoxide dismutase, where a structureless ion diffuses to an enzyme-active site (Sines et al., 1990, 1992). The changes found here are largest at lower ionic strength, at which the steering fields penetrate further out into the solvent. At the physiological ionic strength of 150 mM, the mutations yield rates that are all roughly within a factor of 2 of wild-type. The decreased importance of electrostatic steering at this salt concentration is also evident in the fact that the wild-type rate is only about twice the simulated reaction rate for the case in which no electrostatic interactions are included. The single-sphere model we previously considered, which also used the linearized Poisson-Boltzmann equation, yielded relative rates of the same magnitude as the more complicated model, although there were some notable differences, especially concerning the ionic strength dependence of the relative rates.

Our model was motivated by the desire to have a system that is relatively simple from a computational viewpoint, yet still includes orientational effects and realistic steering fields such that reasonable protein-protein association rates are obtained. Compared with our previous treatment, the electrostatics portion has been improved by using the multigrid-Newton method to solve the full nonlinear Poisson-Boltzmann equation. Given that the algorithm has been shown to scale very favorably with problem size (Holst, 1993; Holst et al., 1994a), a next step would be to solve this equation for the full Fab domain of the HyHEL-5 antibody, rather than just its Fv fragment. Although it is unlikely that this will noticeably change the steering fields because the additional charges are far from the binding site, the extra portion of the protein may possibly induce some observable steric effects. It is also possible to construct a more detailed model of the lysozyme to the point where specific mutations on the antigen can be studied. The resulting computational effort, which would probably require large amounts of CPU time on a massively parallel supercomputer, can be implemented in the manner described above. We also note that the way in which the simulation is now done, wherein the antibody is fixed and rigid, treats the proteins in an asymmetric fashion; this feature ought to be removed or at least tested, perhaps by performing a "reverse" calculation in which the antibody undergoes diffusional motion in the field of the lysozyme. In addition a symmetric calculation with both the antibody and antigen moving, with the evolution of the trajectories in a coordinate system fixed at the antibody, is feasible but computationally expensive.

There are also various physical effects that have not been considered within the framework of these Brownian dynamics studies. It would certainly be useful to perform an investigation of the intermolecular hydrodynamic interactions (Brune and Kim, 1994), with realistic molecular shapes, between antibody and antigen for an actual comparison with the electrostatic steering. It has also been suggested, through analytical solutions of the diffusion equation, that short-range van der Waals forces may be important in keeping two proteins together as they reach the optimum docking configuration (Chou and Zhou, 1982). Finally, atomic-level models can be employed to validate the results from calculations based on continuum approximations. For example, it appears increasingly likely that such models are necessary to explain the extraordinary sensitivity of the HyHEL-5-lysozyme binding affinity on mutations involving the Arg-45 and Arg-68 residues of the lysozyme.

An enormous advantage of Brownian dynamics simulations is the computation of protein-protein reaction rates that can be measured in the laboratory. As demonstrated here and elsewhere, the technique is particularly powerful for probing the effects of various mutations in a given system (Getzoff et al., 1992). The results presented here concerning the antibody mutants can be experimentally tested by performing experiments similar to those already done on the 2B5-cytochrome *c* complex and on altered systems prepared through site-directed mutagenesis. This synthesis of computer modeling using modern parallel and vector architectures and continually improving algorithms together with a growing body of experimental data and an increasing number of x-ray crystal structures can eventually provide the means for understanding protein-protein interactions and the molecular basis of immune response.

We thank J. A. McCammon for providing us with a copy of the UHBD code. This work was supported in part by National Institutes of Health grant R01 GM46535 (subcontract from Texas A & M), and National Science Foundation grant ASC 89-02829. We are grateful to the National Center for Supercomputing Applications and the Pittsburgh Supercomputing Center for allocations of computational resources.

REFERENCES

Allison, S. A., R. J. Bacquet, and J. A. McCammon. 1988. Simulation of the diffusion-controlled reaction between superoxide and superoxide dismutase. II. Detailed models. *Biopolymers.* 27:251–269.

Allison, S. A., J. J. Sines, and A. Wierzbicki. 1989. Solutions of the full Poisson-Boltzmann equation with application to diffusion-controlled reactions. *J. Phys. Chem.* 93:5819–5823.

Bagheri, B., A. Ilin, and R. Scott. 1993. Parallelizing UHBD. University of Houston report.

Brune, D., and S. Kim. 1994. Hydrodynamic steering effects in protein association. *Proc. Natl. Acad. Sci. USA.* 91:2930–2934.

Chou, K. C., and G. P. Zhou. 1982. Role of protein outside active site on the diffusion-controlled reaction of enzyme. *J. Am. Chem. Soc.* 104:1409–1413.

Creighton, T. E. 1982. Proteins: Structures and Molecular Properties. Freeman, New York.

Davis, M. E., J. D. Madura, B. A. Luty, and J. A. McCammon. 1991a. Electrostatics and diffusion of molecules in solution: Simulations with the University of Houston Brownian Dynamics program. *Comp. Phys. Comm.* 62:187–197.

Davis, M. E., J. D. Madura, J. Sines, B. A. Luty, S. A. Allison, and J. A. McCammon. 1991b. Diffusion-controlled enzymatic reactions. *Methods Enzymol.* 202:473–497.

Dickinson, E. 1985. Brownian dynamics with hydrodynamic interactions: the application to protein diffusional problems. *Chem. Soc. Rev.* 14:421–455.

Ermak, D. L., and J. A. McCammon. 1978. Brownian dynamics with hydrodynamic interactions. *J. Chem. Phys.* 69:1352–1360.

Getzoff, E. D., C. L. Fisher, H. E. Page, M. S. Viezzoli, L. Banci, and R. A. Hallewell. 1992. Faster superoxide dismutase mutants designed by enhancing electrostatic steering. *Nature.* 358:347–351.

Hibbits, K. A., D. S. Gill, and R. C. Willson. 1994. Isothermal titration calorimetric study of the association of hen egg lysozyme and the anti-lysozyme antibody HyHEL-5. *Biochemistry.* 33:3584–3590.

Holst, M. J. 1993. Multilevel methods for the Poisson-Boltzmann equation. Ph. D. thesis. Department of Computer Science, University of Illinois at Urbana-Champaign. 103–129.

Holst, M. J., R. E. Kozack, F. Saied, and S. Subramaniam. 1994a. Treatment of electrostatic effects in proteins: multigrid-based solution of the full nonlinear Poisson-Boltzmann equation. *Proteins.* 18:231–245.

Holst, M. J., R. E. Kozack, F. Saied, and S. Subramaniam. 1994b. Protein electrostatics: rapid multigrid-based Newton algorithm for solution of the full nonlinear Poisson-Boltzmann equation. *J. Biomol. Struct. Dyn.* 11: 1437–1445.

Jorgensen, W. L., and J. Tirado-Rives. 1988. The OPLS (optimized potentials for liquid simulations) potential functions for crystals of cyclic peptides and crambin. *J. Am. Chem. Soc.* 110:1657–1669.

Kozack, R. E., and S. Subramaniam. 1993. Brownian dynamics simulations of molecular recognition in an antibody-antigen system. *Protein Sci.* 2:915–926.

Kramers, H. A. 1940. *Physica (Amsterdam).* 7:284–304.

Lavoie, T. B., L. N. W. Kam-Morgan, A. B. Hartman, C. P. Mallett, S. Sheriff, D. G. Saroff, C. R. Mainhart, P. A. Hamel, J. F. Kirsch, A. C.Wilson, and S. J. Smith-Gill. 1989. Structure-function relationships in high-affinity antibodies to lysozyme. *In* The Immune Response to Structurally Defined Proteins: The Lysozyme Model. S. J. Smith-Gill and E. E. Secarz, editors. Adenine Press, New York.

Luty, B. A., R. C. Wade, J. D. Madura, M. E. Davis, J. M. Briggs, and J. A. McCammon. 1993. Brownian dynamics simulations of diffusional encounters between triose phosphate isomerase and glyceraldehyde phosphate: electrostatic steering of glyceraldehyde phosphate. *J. Phys. Chem.* 97:233–237.

Northrup, S. H. 1994. Hydrodynamic motions of large molecules. *Curr. Opin. Struct. Biol.* 4:269–274.

Northrup, S. H., S. A. Allison, and J. A. McCammon. 1984. Brownian dynamics simulation of diffusion-controlled biomolecular reactions. *J. Chem. Phys.* 80:1517–1524.

Northrup, S. H., J. O. Boles, and J. C. Reynolds. 1987. Electrostatic effects in the Brownian dynamics of association and orientation in heme proteins. *J. Phys. Chem.* 91:5991–5997.

Northrup, S. H., and H. P. Erickson. 1992. Kinetics of protein-protein association explained by Brownian dynamics computer simulation. *Proc. Natl. Acad. Sci. USA.* 89:3338–3342.

Northrup, S. H., K. A. Thomasson, C. M. Miller, P. D. Barker, L. D. Eltis, J. G. Guillemette, S. C. Inglis, and A. G. Mauk. 1993. Effects of charged amino acid mutations on the bimolecular kinetics of the reduction of yeast iso-I-ferricytochrome *c* by bovine ferrocytochrome b5. *Biochemistry.* 32: 6613–6623.

Raman, C. S., R. Jemmerson, B. T. Nall, and M. J. Allen. 1992. Diffusion-limited rates for monoclonal antibody binding to cytochrome *c*. *Biochemistry.* 31:10370–10379.

Sharp, K. A. 1994. Electrostatic interactions in macromolecules. *Curr. Opin. Struct. Biol.* 4:234–239.

Sheriff, S., E. W. Silverton, E. A. Padlan, G. H. Cohen, S. J. Smith-Gill, B. C. Finzel, and D. R. Davies. 1987. Three-dimensional structure of antibody-antigen complex. *Proc. Natl. Acad. Sci. USA.* 84: 8075–8079.

Sines, J. J., S. A. Allison, and J. A. McCammon. 1990. Point-charge distributions and electrostatic steering in enzyme-substrate encounter: Brownian dynamics of modified copper-zinc superoxide dismutases. *Biochemistry.* 29:9403–9412.

Sines, J. J., J. A. McCammon, and S. A. Allison. 1992. Kinetic effects of multiple charge modifications in enzyme-substrate reactions: Brownian dynamics simulations of Cu,Zn superoxide dismutase. *J. Comp. Chem.* 13:66–69.

Slagle, S. P., R. E. Kozack, and S. Subramaniam. 1994. Role of electrostatics in antibody-antigen association: anti-hen egg lysozyme/lysozyme complex (HyHEL-5/HEL). *J. Biomol. Struct. Dyn.* 12:439–456.

Smith-Gill, S. J., A. C. Wilson, M. Porter, E. M. Prager, R. J. Feldmann, and C. R. Mainhart. 1982. Mapping the antigenic epitope for a monoclonal antibody against lysozyme. *J. Immunol.* 128:314–322.

Warwicker, J., and H. C. Watson. 1982. Calculation of the electric potential in the active site cleft due to α-helix dipoles. *J. Mol. Biol.* 157:671–679.